Optical and Quantum Electronics (2024) 56:1357
https://doi.org/10.1007/s11082-024-07264-z

High efficiency laser ablation of gold thin film by 2.8 GHz intraburst repetition rate pulses

Emre Hasar[1] · Selin Aşmanoğlu[2] · Fatih Ömer Ilday[3,4] · Parviz Elahi[1,5]

Received: 30 December 2023 / Accepted: 9 July 2024 / Published online: 25 July 2024

Abstract
This work initially presents our progress in developing a 14 W all-polarization-maintaining (PM) Yb-doped fiber laser system. This system can generate bursts with a 2.8 GHz intraburst repetition rate and offers flexibility in burst repetition rates, starting from 100 kHz. The laser produces pulse energies up to 210 nJ, which can be dechirped to approximately 650 fs. Subsequently, we utilized the developed laser in thin film gold processing. We sent up to 6.4 W and employed three different intraburst pulse configurations on a 100 nm-thick gold film coated on glass. We achieved a record gold removal efficiency of 125 μg/W.s using ~5 nJ pulses. Moreover, we determined an ablation pulse energy threshold of approximately 1 nJ, representing the lowest pulse energy to the best of our knowledge.

Keywords Ablation-cooled · GHz fiber laser · Burst mode fiber laser · Gold ablation

1 Introduction

Yb-doped fiber lasers present numerous advantages, including high slope efficiency and excellent beam quality, rendering them versatile tools in a broad spectrum of applications in laser science and technology (Shi et al. 2014; Zervas and Codemard 2014; Zervas 2014; Fermann and Hartl 2013). The burst mode Yb-doped fiber lasers, especially at GHz-range intraburst repetition rate, has been receiving significant attention in recent years (Kerse et al. 2016b; Ma et al. 2023; Han et al. 2022; Bartulevicius et al. 2022; Liu et al. 2023). Burst mode operation, characterized by high peak power and pulse repetition rates within the GHz regime, has the potential to revolutionize various applications, including high-efficient material processing and micromachining (Kerse et al. 2016a; Kalaycıoğlu et al. 2017;

✉ Parviz Elahi
parviz.elahi@ozyegin.edu.tr

[1] Department of Physics, Bogazici University, 34342 Istanbul, Turkey

[2] Department of Physics, Middle East Technical University, 10587 Ankara, Turkey

[3] Faculty of Electrical Engineering and Information Technology, Ruhr University, 44801 Bochum, Germany

[4] Faculty of Physics and Astronomy, Ruhr University, 44801 Bochum, Germany

[5] Department of Natural and Mathematical Sciences, Özyeğin University, 34794 Istanbul, Turkey

Mishchik et al. 2019; Bonamis et al. 2019; Elahi et al. 2018; Schwarz et al. 2021), the ability to produce bursts of ultrashort pulses at a GHz-range pulse repetition rate has enhanced the quality of laser micromachining. Employing GHz bursts of ps or fs laser pulses in ablation introduces a new regime of laser ablation, “ablation cooling," where material removal occurs with minimal heat accumulation (Kerse et al. 2016a). The ablation-cooled laser-treated surfaces have unveiled clearly defined ablation features, signaling a decrease in thermal impact and a noteworthy enhancement in ablation efficiency, measured as the volume of ablated material per the delivered energy.

Focusing on laser gold processing, Smirnov et al. (2022) reported the ablation of a bulk gold in air and water in the range of pulse durations of 0.3–10 ps at 515 nm. Stuart et al. (1996) investigated the ablation threshold of gold by ultrafast laser with different wavelengths and pulse durations. Preuss et al. (1995) investigated the ablation of various metals, including gold, sub-ps at the wavelength of 248 nm. Dittrich et al. (2019) studied the ablation of gold in the air and water at the wavelength around 1 µm for three different laser classes operating at different pulse durations. Using 3 ps-long pulses, they achieved a maximum of about 40 µg/W.s material removal efficiency at about 2.4 J/cm^2. Zhou et al. (2020) studied the ablation threshold of gold film on different substrates irradiated by single pulse ultrafast laser.

In this work, we first present the development of a 14 W Yb-doped all-PM-fiber laser system that generates pulses at a 2.8 GHz repetition rate and operates in a burst mode with a flexible burst repetition rate starting from 100 kHz. The system produces 25 ps-long and 650 fs-long pulses before and after dechirping, respectively. The maximum burst and pulse energies at 100 kHz burst repetition rate comprise 665 pulses per burst (burst duration of 240 ns) is 140 µJ and 210 nJ, respectively. Using our developed fiber laser, we then demonstrated the gold thin film ablation in the ablation-cooled regime. We investigated the ablation efficiency and ablation rate at various burst energies and intraburst pulse numbers.

2 Fiber laser development

Figure 1 illustrates the schematic representation of our fiber laser system. This laser system comprises a passively mode-locked oscillator, followed by three amplification stages, all utilizing optical fibers with a core diameter of 10 µm. We have incorporated a fiber-coupled acousto-optic modulator (AOM) immediately following the first amplification stage to achieve burst operation. The oscillator operates at a pulse repetition rate of 89 MHz, and the power at the rejection port of the polarized beam splitter (PBS), which is placed inside the oscillator, is 52 mW. As depicted in Fig. 2a, the optical spectrum reveals a spectral width of 17 nm. The measured pulse duration is about 2 ps.

52 mW output from the oscillator is directed into a single-mode patchcord collimator. Subsequently, a PM in-line isolator is positioned after the collimator to effectively mitigate any potential issues arising from back reflections. The seed pulses are then directed toward a repetition rate multiplier (RRM) comprising six 3 dB PM fiber optic couplers, increasing the repetition rate to 2.8 GHz. The output power measured from the RRM is 18 mW. Output pulses from the RRM are temporally stretched to approximately 80 ps by passing through 100 ms of single-mode (SM) fiber. The stretched pulses are directed into the initial amplifier stage. This stage is constructed using a 2-m long double-clad (DC), PM Yb-doped (Yb-10/125 PM 1200DC) pumped by an 18 W, wavelength-stabilized multimode diode laser at 976 nm. This pump source is coupled to the

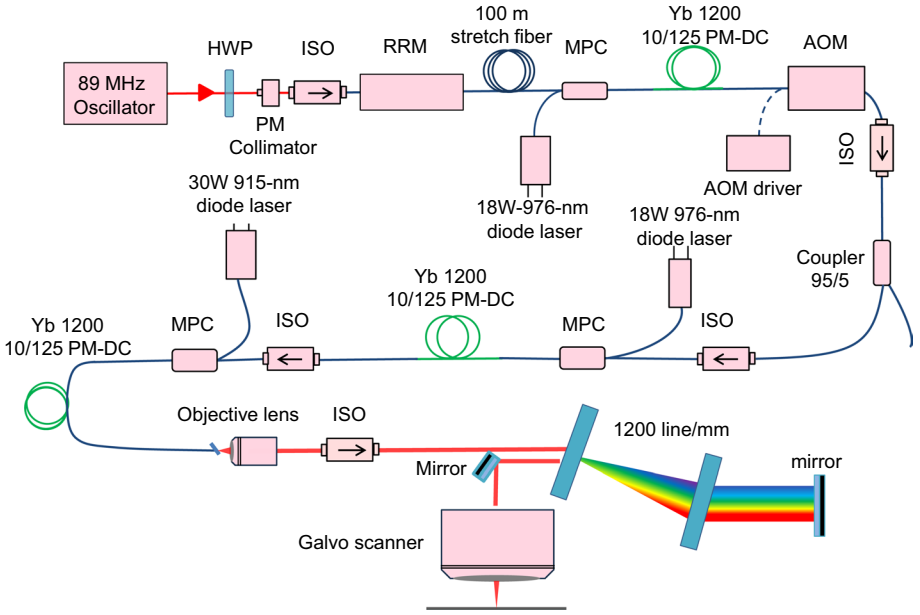

Fig. 1 Schematic diagram of the developed laser and experimental setup. HWP, half wave plate; ISO, isolator; RRM, repetition rate multiplier; AOM, acousto optic modulator; MPC, multimode pump signal combiner

fiber via a multimode pump signal combiner (MPC). The launched pump power is 6 W, and the obtained signal power is 4 W. Next, an in-line acousto optics modulator (AOM) converts the system to burst mode. The insertion loss of the AOM is 2.5 dB with the rise/fall time of 10 ns. The burst pattern is electronically fed to the AOM driver by an arbitrary waveform generator (AWG). For 560 pulses (burst duration of 200 ns) at 100 kHz burst repetition rate (0.02 duty cycle), the output power of the AOM is 45 mW. Figure 2b shows the burst and intraburst pulse trains.

Next, the 45 mW signal, after passing through an inline isolator (PM 10/125, 0.6 dB insertion loss) and a 95%/5% coupler, is amplified to about 2 W in the second cladding-pumped amplifier comprises 2.7-m long double-clad, PM Yb-doped fiber (Yb-10/125 PM 1200DC). The final section of the laser system, the power amplifier, consists of a 30 W multimode pump diode at 915 nm and 5 m-long PM Yb-doped fiber (Yb-10/125 PM 1200DC). In this amplifier stage, the signal boosted from 1.3 to 14 W with a launched pump power of 23 W, yielding a pump-to-signal conversion efficiency of 56%, which is an advancement in terms of average power and fiber core size compared to our previous works e.g., Kerse et al. (2016a). The optical spectra measured at 1.3 W, 8.1 W, and 14 W output powers and the corresponding intensity autocorrelations are shown in Fig. 2c and d. In these measurements, the burst duration is 240 ns (665 pulses in each burst), and the burst repetition rate is 100 kHz. Raman, as a nonlinear effect that enables wavelength conversion, is produced at about 8.0 W (~122 nJ individual pulse energy), as shown in Fig. 2c. The Raman shift is about 13 THz, which corresponds to a shift of around 47 nm at 1040 nm central wavelength. Thus, as depicted in the figure, Raman generation occurs at approximately 1087 nm. As shown in Fig. 2d, the pulse duration before dechirping remains constant at 25 ps at these power levels. The

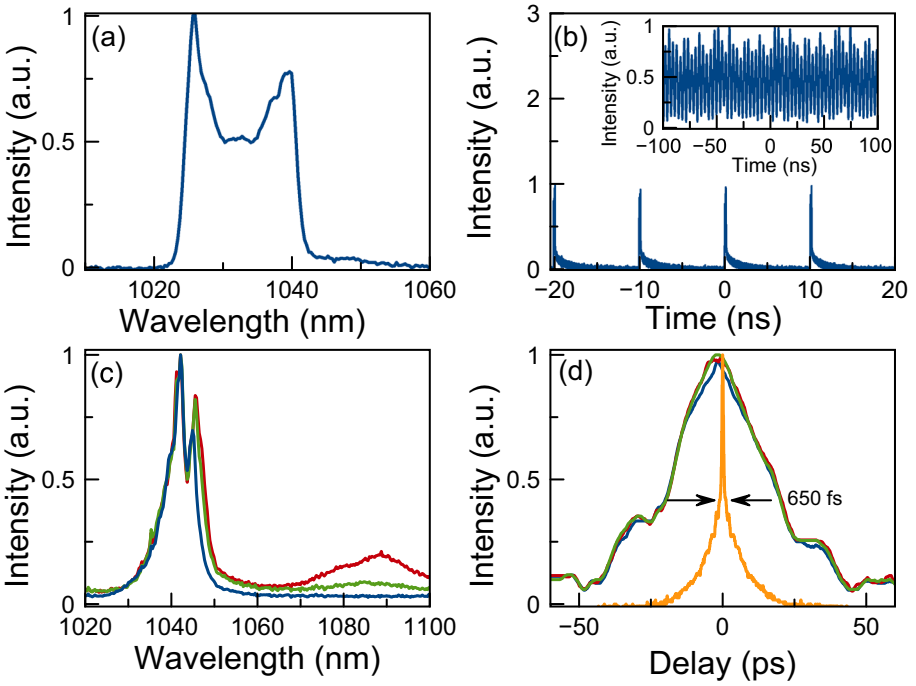

Fig. 2 The measured optical spectrum of the mode-locked oscillator (**a**), the burst train at 100 kHz (inset: 2.8 GHz intrabusrt repetition rate) (**b**), the measured output spectra at 1.3 W (blue), 8.1 W (green), and 14 W (red) at 100 kHz burst repetition rate comprises 665 pulse (**c**), the corresponding intensity autocorrelation along with the compressed pulse (orange) (**d**)

pulses are compressed with a pair of 1200 lines/mm transmission gratings down to 650 fs (Fig. 2d).

3 Ablation of gold thin film

The developed fiber laser has been employed in 100 nm-thickness gold processing. The laser operates with an average output power of 14 W at a burst repetition rate of 100 kHz. The intraburst pulse repetition rate is 2.8 GHz. While the burst repetition rate is adjustable, the laser operates above 100 kHz to minimize amplified spontaneous emission (ASE) (Gürel et al. 2014). At 100 kHz burst repetition rate, maximum individual pulse energy is maintained below 120 nJ to avoid Raman.

A high-power 20X (Thorlabs, 980–1130 nm, NA = 0.40) objective is placed after the gain fiber to collimate the laser beam. To avoid the back reflection, the laser output is directed through a high-power free space isolator with an insertion loss of 1 dB. Before entering the isolator, a half-wave plate is positioned to facilitate polarization control and enhance the transmission efficiency from the isolator. Subsequently, the laser beam is directed to a Galvoscanner (Scanlab basiCube 10), which features an entrance aperture with a diameter of 10 mm and an f-theta lens with a focal length of 57 mm. We measured the laser beam diameter by using an iris diaphragm inserted in front of the laser beam by measuring the diameter of the

iris when the power dropped to $1/e^2$ of the input power. The laser beam diameter is adjusted to reach a diameter of about 8 mm. The beam diameter at the focus, ~ 17 µm at $1/e^2$ maximum intensity, was measured by a CCD camera (AmScope, CMOS, Pixel Size: 1.67µm x 1.67µm). The laser spot size can be calculated as $1.83\frac{\lambda f}{D}$, where $\lambda = 1040$ nm, $D = 8$ mm, and $f = 57$ mm. This results in a spot size of 13.6 µm, leading to an estimated beam quality factor of approximately 1.25 .

The ablation performance of the developed high-power laser was evaluated using glass-coated substrates with a 100 nm layer of gold. To investigate the ablation efficiency, we measured the volume of material removed by individual laser bursts, ensuring no temporal overlap between consecutive bursts, where the bursts were delivered at a repetition rate of 100 kHz. We conducted three distinct burst configurations, containing 230, 460, and 920 pulses, each associated with a range of burst energies starting from 1.24 to 6.30 µJ. The minimum and maximum pulse energies in this experiment are about 1.3 nJ and 27.4 nJ, respectively.

The mean ablation volume was calculated by averaging the measurements from multiple spots (in this case, 10 spots) for each energy level. The corresponding fluence was determined based on the incident burst energy per unit area of the laser spot. The average of the minor and major axes was considered for noncircular spots. The ablation rate (defined as the ablated mass per time [mg/s]) and the ablation efficiency (ablated mass per power per time [µg/W.s]) are calculated.

In this study, we use a simple theoretical model to calculate the crater diameter at different burst energies. The model is illustrated the Fig. 3b. By considering a Gaussian profile laser fluence distribution, when the laser fluence is greater than the ablation threshold fluence, the ablation crater radius is assumed to grow exponentially as follows:

$$F_b = F_{th} \exp\left[2\left(\frac{R}{w_0}\right)^2\right]. \tag{1}$$

where $F_b = E_b/\pi(w_0/2)^2$ [J/cm^2] is the laser fluence, w_0 [µm] is the beam waist, and R [µm] is the ablated raius. The crater radius can be calculated as:

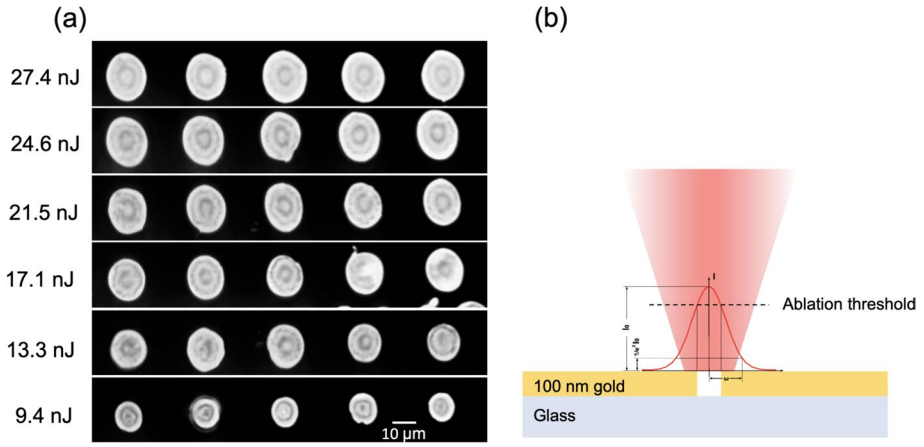

Fig. 3 The microscopic images of the gold removal at different pulse energies with 230 pulses/burst (**a**), the schematic diagram of the laser energy distribution (**b**)

$$R = w_0 \left[\frac{ln\left(\frac{E_b}{E_{th}}\right)}{2} \right]^{\frac{1}{2}} \tag{2}$$

where E_b [J] is the burst energy and E_{th} [J] is the burst energy threshold.

4 Results and discussions

We conducted the single burst-shot experiment with the beam waist at the focus as 17 μm. At 100 kHz burst repetition rate, to avoid any overlap between two adjacent bursts, the speed of galvo scanner has to be greater than 1.7 m/s. Although AOMs typically have power handling limitations, a Pockels cell can also be used after the power amplifier to control the output laser pulses in high-power lasers.The sample is placed precisely at the laser focus using the image of the reflected beam (Polat et al. 2023) and maximizing the intensity of plasma produced in ablation. Figure 4a shows the crater diameter measured at different burst energies for 230, 460, and 920 pulses in each burst. By fitting the Eq. 2, the threshold burst energy for 230, 460, and 920 pulses are calculated as 1.05 μJ, 0.92 μJ, and 1.0 μJ. The corresponding threshold pulse energies are 4.56 nJ, 2.0 nJ, and 1.1 nJ, respectively. We did not observe a significant change in the burst energy threshold with the number of intraburst pulses.

For the thin film gold ablation in the air with the glass substrate, we achieved the threshold fluence of 0.4 J/cm^2 which is close to Dittrich et al. (2019) and Zhou et al. (2020).

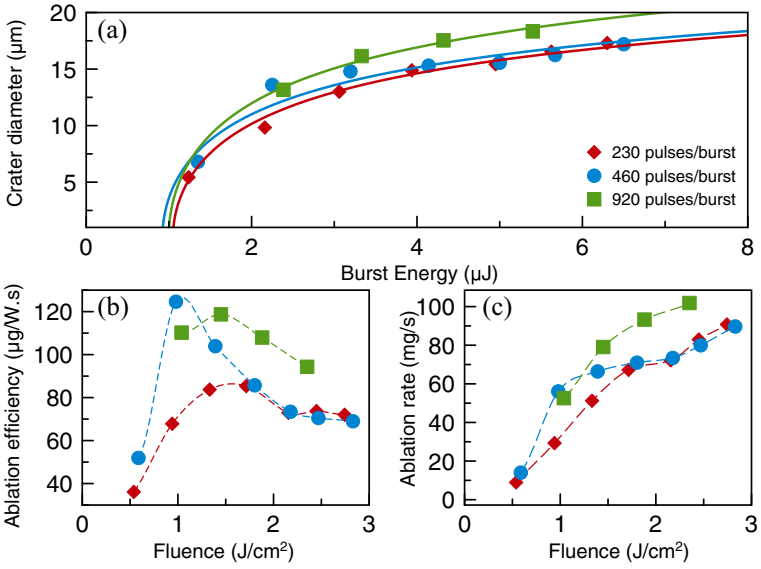

Fig. 4 The crater diameter variation versus burst energy for different intraburst numbers of pulses. The solid curves show the fitting based on Eq.3 (**a**). The ablation efficiency (**b**), and the ablation rate (**c**) versus the burst fluence for different intraburst numbers of pulses

Using 920 pulses, the 1.1 nJ pulse energy threshold is two orders of magnitude lower than in Zhou et al. (2020).

In Fig. 4b and c, the fluence-dependent ablation efficiency and ablation rate with 230, 460, and 920 pulses per burst for gold thin film is presented. The ablation efficiency results can be seen in Fig. 4b. Although the 920 pulses per burst gives a better ablation efficiency in general, the maximum efficiency 124 μg/W.s is achieved by 460 pulses per burst with individual pulse energy 4.9 nJ (2.25 μJ burst energy, 0.98 J/cm^2 fluence, 0.45 W average power). As shown in Fig. 4b, the maximum ablation efficiency obtained for 230 pulses per burst is about 85.3 μg/W.s with individual pulse energy 17.1 nJ (3.9 μJ burst energy, 1.7 J/cm^2 fluence, 0.8 W average power) and the maximum ablation efficiency obtained for 920 pulses per burst is 118.7 μg/W.s with individual pulse energy 3.6 nJ (3.3 μJ burst energy, 1.45 J/cm^2 fluence, 0.66 W average power).

The ablation rate results in Fig. 4c show the ablation rate of the laser which is increasing with the increasing fluence in the range 0.5–3 J/cm^2. Furthermore, the ablation rate of the burst mode, which consists of 920 pulses, is higher than other results within the same fluence range. The maximum ablation rate is obtained as 102×10^3 μg/s for 920 pulses per burst with individual pulse energy 5.87 nJ (5.4 μJ burst energy, 2.35 J/cm^2 fluence, 1.08 W average power). The maximum ablation rate obtained for 230 pulses per burst is 90.7×10^3 μg/s with individual pulse energy 27.4 nJ (17.3 μJ burst energy, 2.7 J/cm^2 fluence, 1.26 W average power). The maximum ablation rate obtained for 460 pulses per burst is 89.7×10^3 μg/s with individual pulse energy 14.1 nJ (6.5 μJ burst energy, 2.8 J/cm^2 fluence, 1.3 W average power).

5 Conclusion

We first presented the development of a 2.8 GHz pulse repetition rate, 14 W average power, all PM fiber laser systems operating in the burst mode regime and then its application in the ablation of gold film coated on glass. The system produces 25 ps-long and 650 fs-long pulses before and after the grating. To investigate the ablation efficiency and ablation rate, we performed the experiment within a fluence range from 0.5–3 J/cm^2. We measured the minimum required pulse energy for ablating the gold thin film as 1.1 nJ with 920 pulses per burst. With 920 pulses per burst, we achieve ~ 120 μg/W.s and ~ 100 mg/s at ~ 1.5 J/cm^2 and ~ 2.3 J/cm^2 burst fluences, respectively. When comparing the efficiency of the three different burst modes operating in the same fluence range, the burst with more pulses has higher ablation efficiency, as seen in Fig. 4c. At the same energy fluence, we achieved higher efficiency than Dittrich et al. (2019). For instance, at 1.45 J/cm^2 we obtained about 120 μg/W.s ablation efficiency (Fig. 4b) and about 80 mg/s ablation rate (Fig. 4c). These values are about 3 times and 6 times higher, respectively than the ablation efficiency and ablation rate of the gold thin film in the air using ps-long pulses in previous results (Dittrich et al. 2019). Our studies indicate promising possibilities for applying GHz-range fiber laser technology in various industry technologies. This especially extends to their use in industrial laser-material processing, which high-energy solid-state or hybrid lasers have traditionally dominated.

Acknowledgements This work was supported by TÜBITAK under projects numbered 121F392 and the European Research Council (ERC) grant "UniLase" (grant agreement 101055055). The authors thank Hamit Kalaycıoğlu, Dinizhan Koray Kesim, and Murat Sozen. PE thanks his former University, Bogazici University.

Funding Open access funding provided by the Scientific and Technological Research Council of Türkiye (TÜBİTAK). This work was supported by TÜBITAK under projects numbered 121F392 and the European Research Council (ERC) grant "UniLase" (grant agreement 101055055).

Declarations

Conflict of interest The authors have not disclosed any competing interests.

References

Bartulevicius, T., Lipnickas, M., Petrauskiene, V., Madeikis, K., Michailovas, A.: 30 W-average-power femtosecond NIR laser operating in a flexible GHz-burst-regime. Opt. Express **30**(20), 36849–36862 (2022)

Bonamis, G., Mishchick, K., Audouard, E., Hönninger, C., Mottay, E., Lopez, J., Manek-Hönninger, I.: High efficiency femtosecond laser ablation with gigahertz level bursts. J. Laser Appl. **31,** 022205 (2019)

Dittrich, S., Streubel, R., McDonnell, C., Huber, H.P., Barcikowski, S., Gökce, B.: Comparison of the productivity and ablation efficiency of different laser classes for laser ablation of gold in water and air. Appl. Phys. A **125**, 1–10 (2019)

Elahi, P., Akçaalan, Ö., Ertek, C., Eken, K., Ilday, F.Ö., Kalaycoğlu, H.: High-power Yb-based all-fiber laser delivering 300 fs pulses for high-speed ablation-cooled material removal. Opt. Lett. **43**(3), 535–538 (2018)

Fermann, M.E., Hartl, I.: Ultrafast fibre lasers. Nat. Photonics **7**(11), 868–874 (2013)

Gürel, K., Elahi, P., Budunoğlu, L., Şenel, Ç., Paltani, P., Ilday, F.: Prediction of pulse-to-pulse intensity fluctuation characteristics of high power ultrafast fiber amplifiers. Appl. Phys. Lett. **105,** 011111 (2014)

Han, M., Xu, Z., Shu, X.: Gigahertz bursts with tunable pulse interval and pulse number based on sinusoidal saturable absorption. Opt. Fiber Technol. **74**, 103130 (2022)

Kalaycıoğlu, H., Elahi, P., Akçaalan, Ö., Ilday, F.Ö.: High-repetition-rate ultrafast fiber lasers for material processing. IEEE J. Sel. Top. Quantum Electron. **24**(3), 1–12 (2017)

Kerse, C., Kalaycıoğlu, H., Elahi, P., Çetin, B., Kesim, D.K., Akçaalan, Ö., Yavaş, S., Aşık, M.D., Öktem, B., Hoogland, H.: Ablation-cooled material removal with ultrafast bursts of pulses. Nature **537**(7618), 84–88 (2016)

Kerse, C., Kalaycıoğlu, H., Elahi, P., Akçaalan, Ö., Ilday, F.Ö.: 3.5-GHz intra-burst repetition rate ultrafast Yb-doped fiber laser. Opt. Commun. **366**, 404–409 (2016)

Liu, S., Zhang, B., Bu, Y., Zhao, D., Zhu, X., Yang, L., Hou, J.: High energy and high peak power GHz burst-mode all-fiber laser with uniform envelope and tunable intra-burst pulses. High Power Laser Sci. Eng. **11**, 1–18 (2023)

Ma, J., Liu, H., Chen, Y., Zhang, N., Shum, P.P.: Generation of 35 fs, 20 μj, GHz pulse burst by hybrid fiber amplification technique. Opt. Express **31**(21), 34224–34231 (2023)

Mishchik, K., Bonamis, G., Qiao, J., Lopez, J., Audouard, E., Mottay, E., Hönninger, C., Manek-Hönninger, I.: High-efficiency femtosecond ablation of silicon with GHz repetition rate laser source. Opt. Lett. **44**(9), 2193–2196 (2019)

Polat, C., Yapici, G.N., Elahi, S., Elahi, P.: High-precision laser focus positioning of rough surfaces by deep learning. Opt. Lasers Eng. **168**, 107646 (2023)

Preuss, S., Demchuk, A., Stuke, M.: Sub-picosecond UV laser ablation of metals. Appl. Phys. A **61**, 33–37 (1995)

Schwarz, S., Rung, S., Esen, C., Hellmann, R.: Enhanced ablation efficiency using GHz bursts in micromachining fused silica. Opt. Lett. **46**(2), 282–285 (2021)

Shi, W., Fang, Q., Zhu, X., Norwood, R.A., Peyghambarian, N.: Fiber lasers and their applications. Appl. Opt. **53**(28), 6554–6568 (2014)
Smirnov, N., Kudryashov, S., Rudenko, A.A., Nastulyavichus, A., Ionin, A.: Ablation efficiency of gold at fs/ps laser treatment in water and air. Laser Phys. Lett. **19**(2), 026001 (2022)
Stuart, B.C., Feit, M.D., Herman, S., Rubenchik, A.M., Shore, B.W., Perry, M.D.: Optical ablation by high-power short-pulse lasers. JOSA B **13**(2), 459–468 (1996)
Zervas, M.N.: High power ytterbium-doped fiber lasersâ€ fundamentals and applications. Int. J. Mod. Phys. B **28**(12), 1442009 (2014)
Zervas, M.N., Codemard, C.A.: High power fiber lasers: A review. IEEE J. Sel. Top. Quantum Electron. **20**(5), 219–241 (2014)
Zhou, S., Zhao, K., Shen, H.: Ablation of gold film on different substrates by ultrafast laser. Opt. Laser Technol. **132**, 106495 (2020)